SUPPORTING INFORMATION

A new series of lanthanide-based complexes with bis(hydroxy)benzoxaborolone ligand: Synthesis, crystal structure, magnetic and optical properties.

Ahmad Abdallah, Carole Daiguebonne*, Yan Suffren, Guillaume Calvez, Kevin Bernot and Olivier Guillou*.

Univ Rennes, INSA Rennes, CNRS UMR 6226 "Institut des Sciences Chimiques de Rennes", F-35708 Rennes, France.

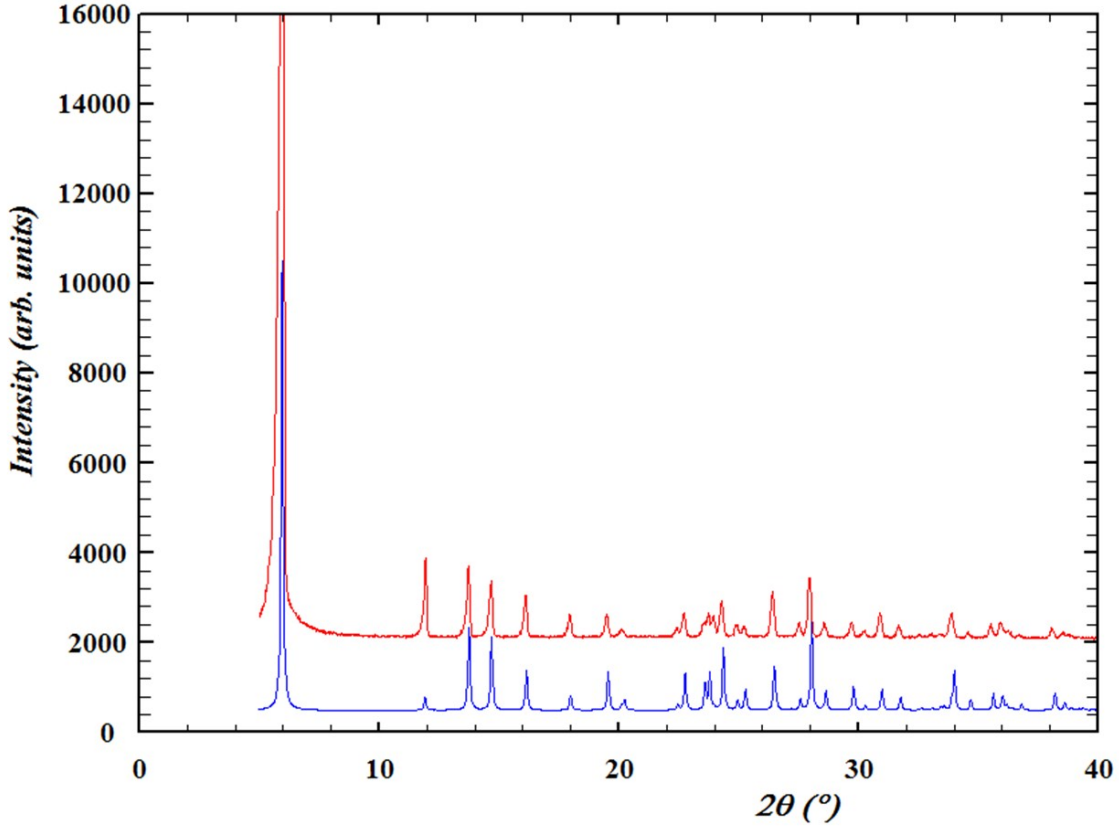

Figure S1. Experimental (red) and simulated from crystal structure (blue) X-ray powder diffraction diagrams of Na(o-cpb) H_2O.

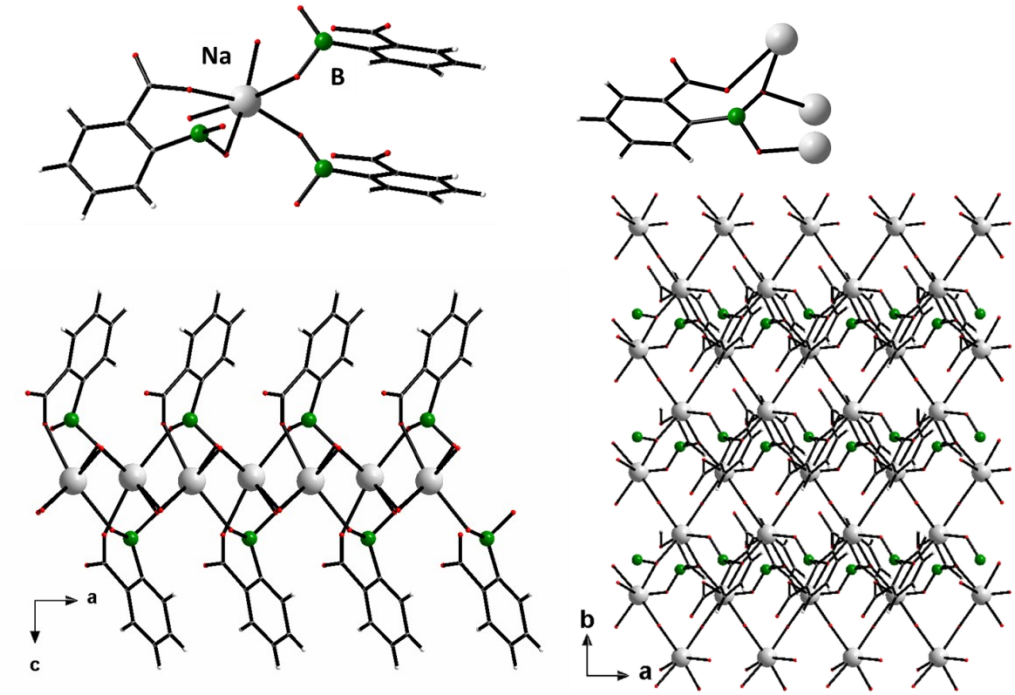

Figure S2. Projection views of the Na^+ ion neighborhood (top left), the binding mode of the ligand (top right), a chain-like molecular motif (bottom left) and the 2D molecular framework (bottom right) for Na(o-cpb)·H_2O. Sodium, boron, oxygen and hydrogen atoms are drawn in grey, green, red and white balls, respectively.

There is only one crystallographically independent Na atom in the crystal structure. It is coordinated to six oxygen atoms that form a slightly distorted octahedron: three from three different -$B(OH)_2$ groups, one from a –COO^- group and two from coordination water molecules. There is only one crystallographically independent ligand as well. Its carboxylate function is deprotonated. It is bound to three different Na^+ ions. This leads to the formation of molecular chains decorated by ligands that spread along the *a*-axis. These molecular chains are linked to each other by aquo-bridges that involve the coordination water molecule which finally produce a 2D molecular framework spreading parallel to the (*ab*) plane.

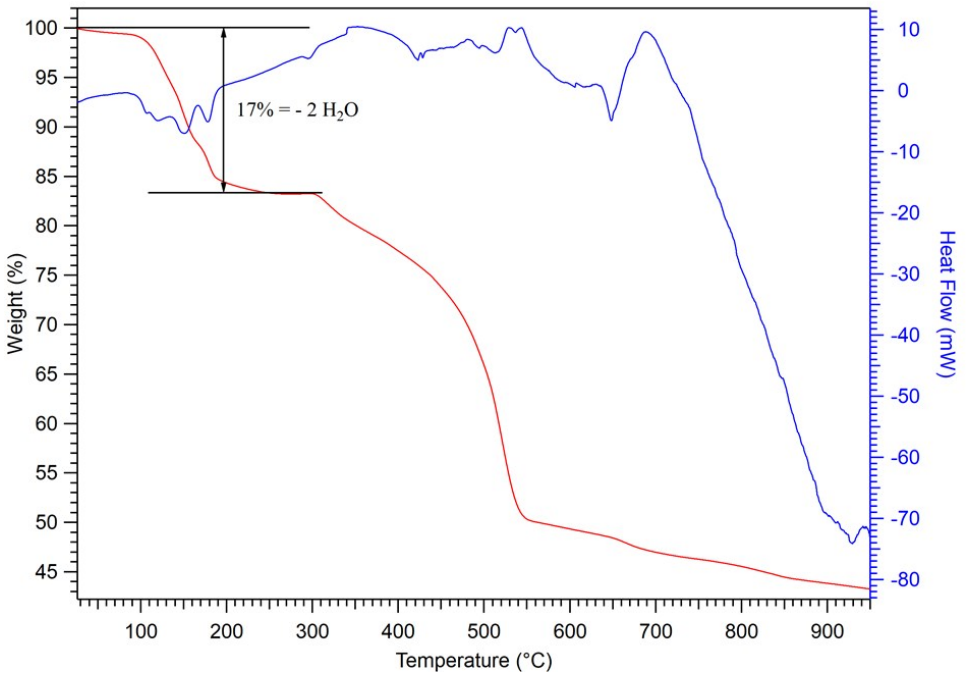

Figure S3. TGA/DSC curves of Na(o-cpb) H_2O.

Thermal analyses indicate a weight loss between 20°C and 200°C that corresponds to two water molecules departure. This weight loss (17%) corresponds to the departure of 2 water molecules: the coordination water molecule and a second water molecule due to the dehydration of the -$B(OH)_2$ group.

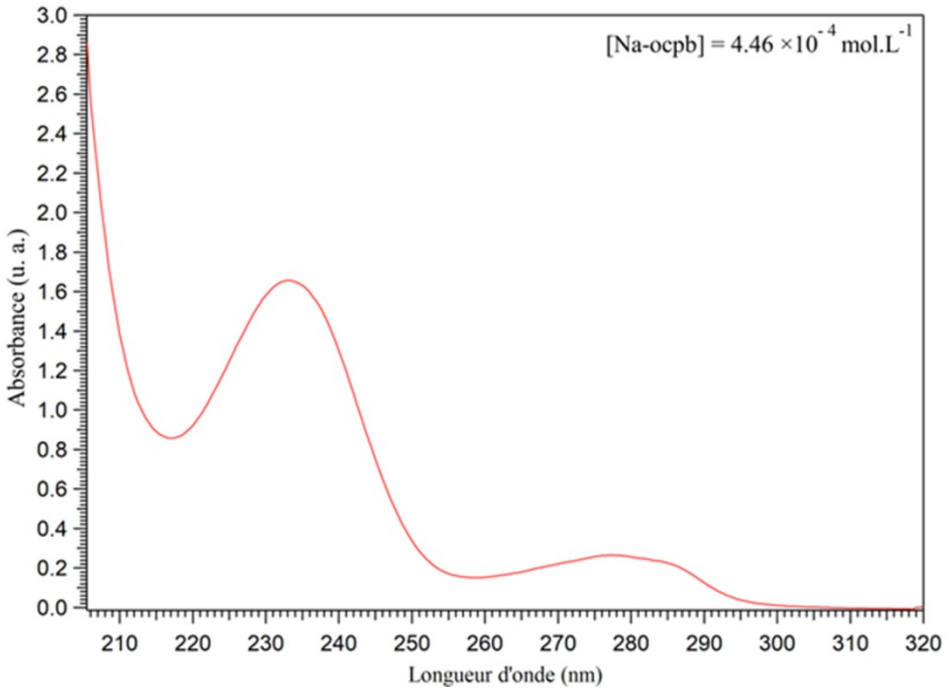

Figure S4. UV-vis liquid-state absorption spectrum of an aqueous diluted solution of Na(o-cpb) H_2O.

Liquid-state absorption spectrum of a diluted aqueous solution of Na(o-cpb)·H_2O (4.46 x 10^{-4} mol.L^{-1}) has been recorded at room-temperature. It shows two broad absorption bands centered at 230 nm and 277 nm, respectively. Corresponding molar absorption coefficients are 3700 $mol^{-1}.cm^{-1}$ and 580 $mol^{-1}cm^{-1}$, respectively. These values are in agreement with those already reported for other benzene-poly-carboxylate ligands.

Table S1. Average measured cell parameters for $[Ln_2(C_7H_5O_2)_4(C_7O_4H_6B)_2\cdot 4H_2O]$ with Ln = Eu-Dy

Ln	*a* (Å)	*b* (Å)	*c* (Å)	*α* (°)	*β* (°)	*γ* (°)
Eu	9.34(2)	16.00(2)	16.19(2)	107.5(5)	90.2(5)	98.0(5)
Gd	9.33(2)	16.03(2)	16.17(2)	107.2(5)	90.0(5)	97.0(5)
Tb	9.35(2)	15.98(2)	16.20(2)	107.5(5)	90.5(5)	97.6(5)
Dy	9.34(2)	16.04(2)	16.21(2)	107.9(5)	89.8(5)	98.0(5)
Tb (Solved crystal structure)	9.3329(13)	16.012(2)	16.212(2)	107.789(5)	90.226(5)	97.585(5)

Table S2. Elemental analyzes* of $[Ln_2(C_7H_5O_2)_4(C_7O_4H_6B)_2\cdot 4H_2O]$ with Ln = Eu-Dy

Ln	Eu	Gd	Tb	Dy
MW ($g.mol^{-1}$)	1190	1200	1204	1211
% Ln found (calc.)	25.4 (25.5)	26.3 (26.2)	26.4 (26.4)	26.7 (26.8)
% C found (calc.)	42.5 (42.4)	42.0 (42.0)	42.0 (41.9)	41.5 (41.6)
% H found (calc.)	3.4 (3.4)	3.2 (3.3)	3.2 (3.3)	3.3 (3.3)
% B found (calc.)	1.7 (1.8)	1.9 (1.8)	1.8 (1.8)	1.9 (1.8)
% O found (calc.)	27.0 (26.9)	27.6 (27.7)	26.6 (26.6)	26.5 (26.4)

C and H contents have been measured by conventional combustion analysis. B and Ln contents have been measured by ICP.

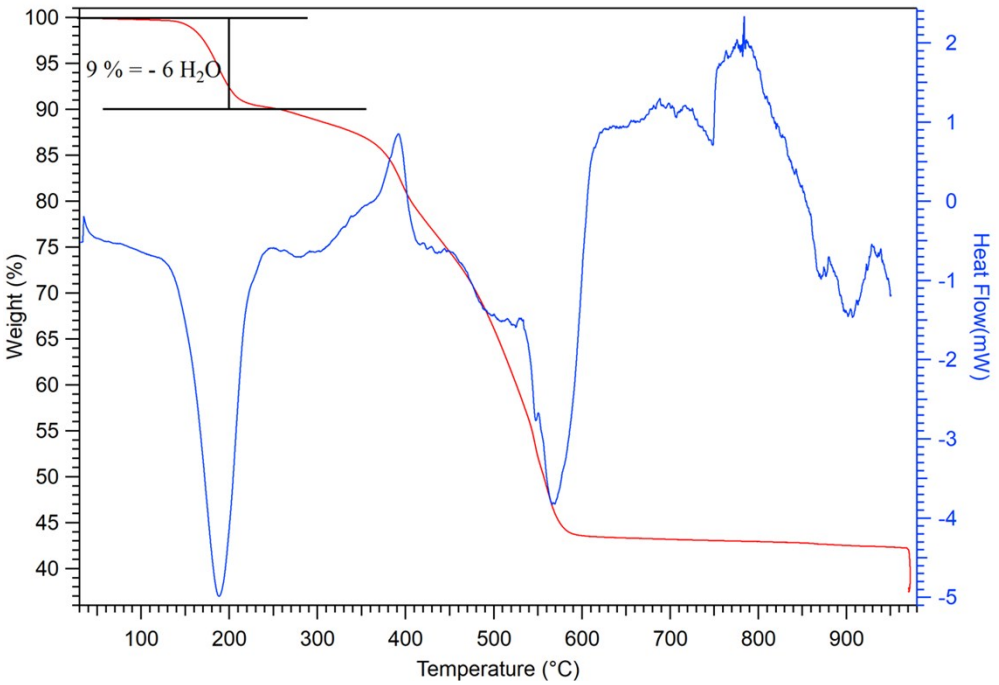

Figure S5. Thermal analysis (TG/TD) of $[Tb_2(C_7H_5O_2)_4(C_7O_4H_6B)_2 \cdot 4H_2O]$.

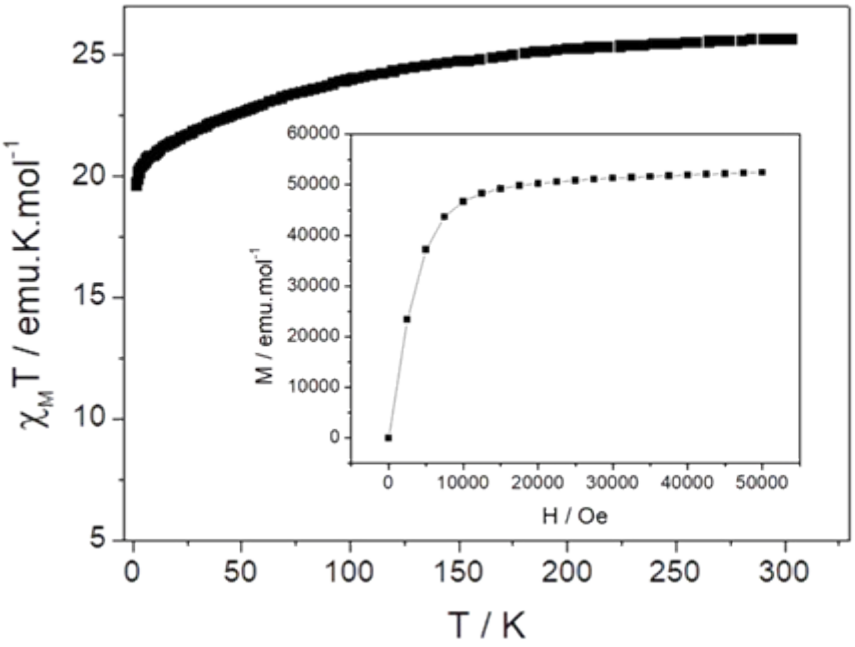

Figure S6. Temperature dependence of $[Dy_2(C_7H_5O_2)_4(C_7O_4H_6B)_2 \cdot 4H_2O]$ measured with a static dc field of 1000 Oe. In inset, the field dependence of the magnetization measured at 2 K.

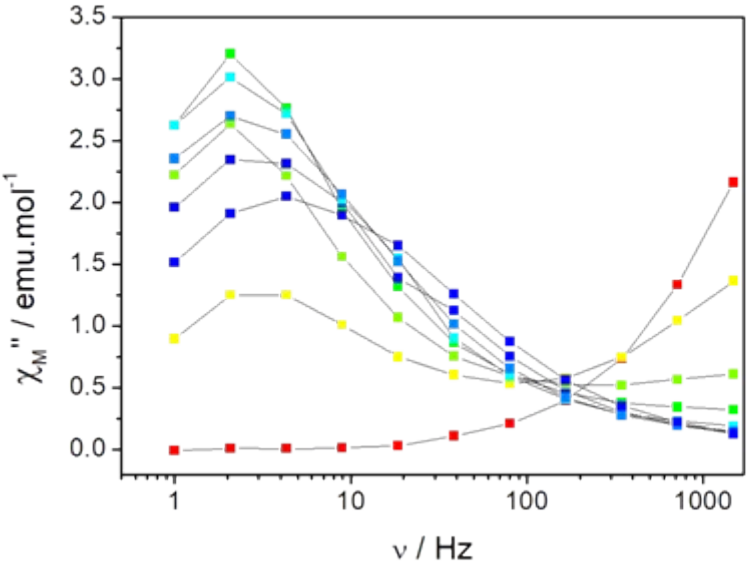

Figure S7. Field dependence of the out-of phase magnetic susceptibility χ_M" of $[Dy_2(C_7H_5O_2)_4(C_7O_4H_6B)_2 \cdot 4H_2O]$ measured at 2 K from 0 Oe (red) to 3200 Oe (blue).

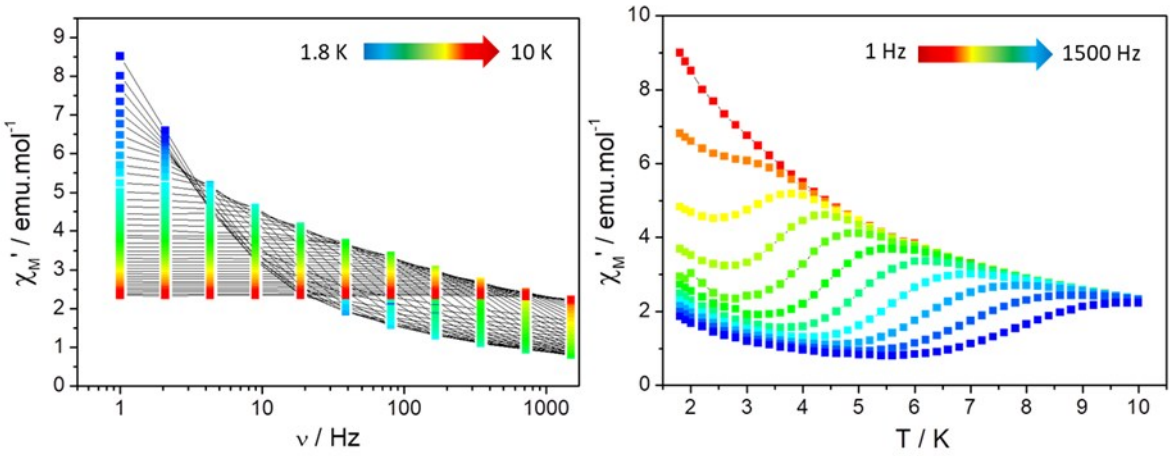

Figure S8. Frequency (left) and temperature dependence (right) of the in-phase magnetic susceptibility χ_M' of $[Dy_2(C_7H_5O_2)_4(C_7O_4H_6B)_2 \cdot 4H_2O]$ measured with a static magnetic field H_{dc} = 1200 Oe.

Table S3: Continuous Shape Measurements (CShM) for $[Dy_2(C_7H_5O_2)_4(C_7O_4H_6B)_2 \cdot 4H_2O]$. The lower is the CShM value, the better is the agreement with the given coordination polyhedron.

Coordination geometry (site symmetry)	Triangular dodecahedron (D_{2d})	Bi-augmented trigonal prism (C_{2v})	Square antiprism (D_{4d})
Dy1 CShM	**2.099**	3.013	3.217
Dy2 CShM	**2.102**	3.008	3.190

Table S4: Relaxation times extracted for $[Dy_2(C_7H_5O_2)_4(C_7O_4H_6B)_2 \cdot 4H_2O]$ with H_{dc} = 1200 Oe.

T(K)	τ (μs)	T(K)	τ (μs)
1.8	91681	5	2133
1.9	85470	5.2	1665
2	77626	5.4	1305
2.2	65634	5.6	1039
2.4	55923	5.8	837
2.6	46862	6	680
2.8	38101	6.2	558
3	30209	6.4	460
3.2	24037	6.6	378
3.4	18694	6.8	314
3.6	14306	7	262
3.8	10787	7.2	226
4	8530	7.4	189
4.2	6086	7.6	164
4.4	4632	7.8	142
4.6	3539	8	125
4.8	2741	8.2	109

Table S5: Adiabatic (χ_S), isothermic (χ_T) susceptibility values and relaxation times distribution (α) extracted for [Dy(o-cpb)] with H_{dc} = 1200 Oe.				
T(K)	χ_S	χ_T	α	R^2
2	2.0768	10.80033	0.20752	0.88844
2.2	2.1017	9.69302	0.16342	0.90952
2.4	1.83863	9.02099	0.17523	0.92302
2.6	1.34872	9.21003	0.31142	0.95483
2.8	1.2774	8.41315	0.28862	0.95389
3	1.19095	7.74779	0.26727	0.95063
3.2	1.134	7.17779	0.24745	0.95189
3.4	1.07832	6.69773	0.22702	0.95326
3.6	1.02292	6.27302	0.20672	0.95454
3.8	0.97338	6.01024	0.19688	0.96692
4	0.93355	5.646	0.16985	0.96428
4.2	0.88483	5.32809	0.15459	0.97173
4.4	0.84802	5.07241	0.13306	0.97409
4.6	0.81588	4.85183	0.12258	0.98123
4.8	0.81144	4.6554	0.10197	0.99149
5	0.76121	4.48777	0.10461	0.97825
5.2	0.75932	4.31411	0.08594	0.99603
5.4	0.71004	4.16319	0.08727	0.99451
5.6	0.66056	4.01087	0.10592	0.95319
5.8	0.67923	3.8881	0.07686	0.99733
6	0.62457	3.46761	0.06764	0.99707
6.2	0.60559	3.36578	0.06679	0.99821
6.4	0.60009	3.26464	0.06355	0.99859
6.6	0.58821	3.1695	0.06023	0.99845
6.8	0.57461	3.08105	0.06091	0.99908
7	0.58819	2.99655	0.05457	0.99896
7.2	0.5942	2.91712	0.05187	0.99937
7.4	0.5688	2.84244	0.05565	0.99695
7.6	0.59117	2.76917	0.04925	0.99963
7.8	0.61557	2.70093	0.04179	0.99924
8	0.6264	2.63515	0.03933	0.99606
8.2	0.68019	2.57292	0.0204	0.99822
8.4	0.61634	2.51327	0.03084	0.99673
8.6	0.70059	2.45488	0.01031	0.99598
8.8	0.51736	2.40641	0.05007	0.99282
9	0.66733	2.30089	0.01076	0.99944